
**ELECTRICAL AND MAGNETIC
PROPERTIES**

Interlayer Interaction and Coercivity of Three-Layer Films Obtained by Chemical Deposition

A. V. Chzhan^{a, b, *}, V. A. Orlov^{a, c}, and M. N. Volochaev^c

^a *Siberian Federal University, Krasnoyarsk, 660041 Russia*

^b *Krasnoyarsk State Agrarian University, Krasnoyarsk, 660049 Russia*

^c *Kirensky Institute of Physics, Siberian Branch, Russian Academy of Sciences, Krasnoyarsk, 660036 Russia*

**e-mail: avchz@mail.ru*

Received June 9, 2023; revised July 31, 2023; accepted August 17, 2023

Abstract—The results of experimental and theoretical studies of the coercivity and the dipole coupling field of the hysteresis loop on the thickness of the nonmagnetic interlayer in magnetic films, which are obtained via chemical deposition, are presented. Using model calculations based on the Landau–Ginzburg equations, the exchange interactions between magnetic layers with the participation of atoms from the nonmagnetic interlayer are studied. The resulting expression for the dipole coupling field describes well the exponential changes in the dipole coupling field as a function of the interlayer thickness in structures with both soft magnetic layers and layers with significantly different values of the coercivity.

Keywords: multilayer magnetic films, interlayer interaction, dipole coupling field, coercivity

DOI: 10.1134/S0031918X23601804

INTRODUCTION

The increased interest in three-layer magnetic films is associated with unusual phenomena in systems that are of fundamental importance and open up new opportunities for the practical application of this type of materials. The most impressive effects observed in three-layer films with a nonmagnetic metal interlayer are the giant magnetoresistance (GMR) [1] and the inverse effect with respect to it, in which an electric current leads to a controlled magnetization reversal in domains [2, 3]. Along with this, multilayer structures are promising for creating new materials with improved soft magnetic properties. Thus, three-layer permalloy-based films with a thin nonmagnetic interlayer have a much lower coercive force [4, 5] than monolayer films of the same thickness and their switching speed is much higher [6]. Such materials are in demand for creating thin-film magnetic heads for recording and reading information from hard disks [7] or magnetic-flux amplifiers in high-frequency devices [8]. Investigations show that one of the main roles in these phenomena is played by the type and thickness of the nonmagnetic interlayer, which determine the character of interaction of the magnetic layers.

The objective of this study is to elucidate the physical mechanisms that cause the interaction between the magnetic layers in three-layer films, which were obtained by the chemical deposition, in the region of small thicknesses of the nonmagnetic interlayer.

EXPERIMENTAL RESULTS

The three-layer films were obtained by the chemical deposition of Co ions together with P on a glass substrate at a temperature of 100°C, which was maintained with an accuracy of 0.01°C. The used method makes it possible to create magnetic layers in different crystalline Co modifications: in the amorphous low-coercive or polycrystalline high-coercive states using a change in the acidity of the working solutions [9].

In this study, three-layer films of two types were investigated, which differed in the crystal structure of the lower magnetic layer. The films of the first type consisted of a low-coercive amorphous $\text{Co}_{1-0.10}\text{P}_{0.10}$ (100 nm) alloy/amorphous $\text{Ni}_{1-0.17}\text{P}_{0.17}(\text{t})$ /hard magnetic crystalline $\text{Co}_{1-0.04}\text{P}_{0.04}$ (40nm) with a coercive force of 500 Oe. The samples of the second type consisted of amorphous $\text{Co}_{1-0.10}\text{P}_{0.10}$ (100 nm)/amorphous $\text{Ni}_{1-0.17}\text{P}_{0.17}(\text{t})$ /amorphous $\text{Co}_{1-0.10}\text{P}_{0.10}$ (100 nm).

The intermediate layer obtained from an amorphous Ni–P alloy is paramagnetic due to the high phosphorus content of ~17 at % (such an alloy changes from the ferromagnetic to paramagnetic state at concentrations of P > 13.7 at % [10]).

Figure 1 shows an image of the cross section of a sample with upper amorphous and lower polycrystalline Co–P alloys, which was obtained using transmission electron microscopy at an FIP FB-2100 (Hitachi) facility using the focused ion beam technique [11]. The difference in the contrasts of the layers is

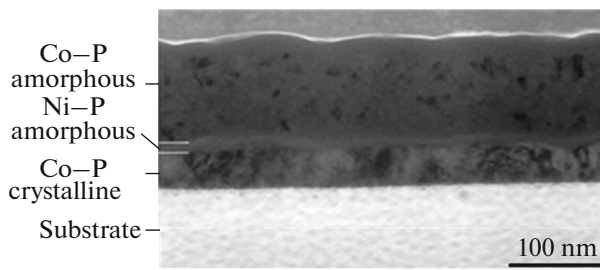


Fig. 1. Cross-sectional view of a three-layer Co–P(amorphous)/Ni–P/Co–P(cryst.) film. The layer above the film corresponds to a protective mask.

explained by their different crystal structures. In the lower polycrystalline layer, crystallites are oriented differently relative to the electron beam; therefore, some of them scatter the electron beam more intensively. Darker areas in the upper amorphous layer are associated with the presence of the nanocrystalline phase.

Electron-microscope studies were performed on the equipment of the Krasnoyarsk Regional Center for Collective Use (Federal Research Center, Krasnoyarsk Scientific Center, Siberian Branch, Russian Academy of Sciences).

The thicknesses of the layers were determined by the X-ray fluorescence analysis [12] according to the deposition time and the growth rate. The error was within 20%. The hysteresis loops were determined using the meridional Kerr magneto-optical effect with a magnetic-field frequency of 0.01 Hz at room temperature.

Figure 2 shows the minor hysteresis loop corresponding to the magnetization reversal of the soft magnetic layer at $H < H_c^h$, where H_c^h is the coercive force of the hard magnetic layer. The value of the dipole coupling

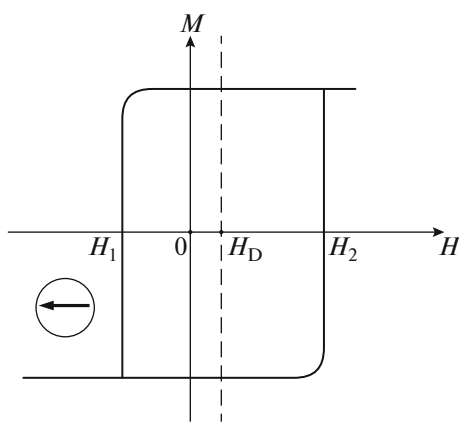


Fig. 2. Minor hysteresis loop corresponding to the magnetization reversal of the soft magnetic layer. The arrow indicates the magnetization direction of the hard magnetic layer.

field H_D was assumed to be equal to $(H_1 + H_2)/2$, where H_1 and H_2 are the critical fields corresponding to the ascending and descending branches of the hysteresis loop. The dipole coupling field of the hysteresis loop against the magnetization of the hard magnetic layer indicates the ferromagnetic nature of the interaction between the layers or its positive sign.

The coercive force H_c in films with a hard magnetic layer was determined as the half-width of the hysteresis loop corresponding to the magnetization reversal of the soft magnetic layer at $H > H_c^h$. The hysteresis loops that correspond to such cycles are shown in the upper part of Fig. 3.

As shown in Fig. 3, with a change in the interlayer thickness t from 0 to 1 nm, the H_D value experiences a sharp drop from 52 to 9.7 Oe, while the H_c value decreases from 120 to 20 Oe.

In samples with soft magnetic layers, the presence of an interlayer also leads to a dipole coupling field of the hysteresis loop, which is observed on particular magnetization-reversal cycles at $H < H_s$, where H_s is the saturation field. As shown in Fig. 4, as the thickness of the interlayer increases, H_D first grows from 0 to 4 Oe and then decreases, becomes negative at $t > 1.8$ nm, and vanishes at $t > 8$ nm.

A dipole coupling field of the hysteresis loop indicates different coercive forces of the magnetic layers, although they have the same composition and thickness: the lower layer occurs to be more highly coercive

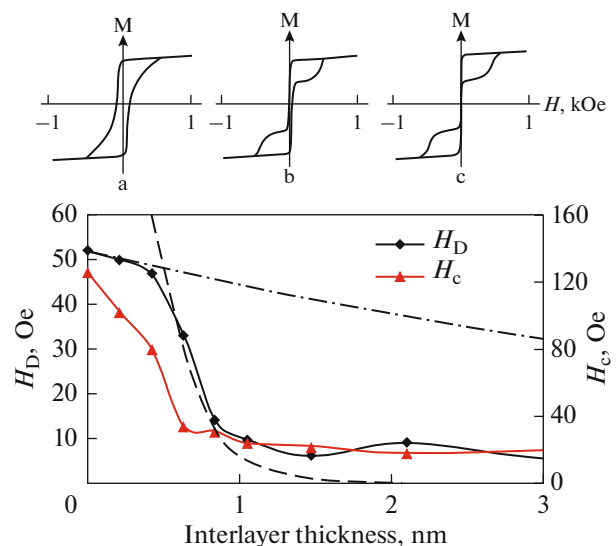


Fig. 3. The upper part includes the hysteresis loops for different interlayer thicknesses: (a) 0, (b) 0.6, and (c) 2 nm. The lower part is the dependences of the dipole coupling field and the coercive force of the soft magnetic layer in CoP(amorphous)/NiP/CoP(cryst.) films on the interlayer thickness. The dashed–dotted and dashed lines show the theoretical curves for the shear field obtained from Eqs. (1) and (8), respectively.

than the upper one due to the influence of the substrate. The change in the H_D sign to negative is explained by the magnetostatic interaction between the magnetic layers, which manifests itself when the ferromagnetic coupling decreases.

The coercive force in the described films was determined from the half-width of the hysteresis loop obtained at $H > H_S$, where H_S is the saturation field. The form of the hysteresis loops corresponding to such a magnetization reversal is shown in the upper part of Fig. 4. The change of H_c as a function of t , as well as the change of H_D , is a nonmonotonic dependence. H_c decreases from 9.5 to 1.4 Oe with the growth of t from 0 to 2 nm and then increases to 3.3 Oe at $t \sim 8$ nm (Fig. 4).

THEORETICAL JUSTIFICATION OF THE RESULTS

The interlayer interaction of the positive sign in a three-layer film with a metal interlayer can be caused by several factors:

- an indirect exchange through conduction electrons (RKKY interaction);
- roughness of the boundary layer (Neel mechanism) [13];
- imperfections of the interlayer due to its discontinuity and varying thickness over the film area [4];
- indirect interaction between the FM layers due to the spin polarization of the atoms in the paramagnetic interlayer due to the influence of the boundary atoms of the FM layers—an effect similar to that observed in strong paramagnets [14, 15].

The RKKY interaction is characterized by a pronounced alternating effective exchange between the FM layers, which does not correspond to the experimental results (see Fig. 3).

In the Neel model, the roughness at the upper and lower boundaries of the intermediate layer is approximated by a harmonic function depending on the amplitude h and the roughness length λ . The amplitude of the coupling field in this case is determined by the expression [16, 17]:

$$H_D = \frac{\pi^2 h^2}{\sqrt{2} \lambda t_f} M_s \exp\left(-\frac{2\pi\sqrt{2}t}{\lambda}\right), \quad (1)$$

where M_s and t_f are the magnetization and thickness of the low-coercive layer, and t is the interlayer thickness.

The roughness parameters were determined in pixels directly on the cross-sectional image of the film (Fig. 1) using the Image J program and then were converted to nanometers. The average sizes of h and λ were 4 ± 1 and 55 ± 20 nm, respectively. The expected change in the dipole coupling field as a function of the interlayer thickness that was found from (1) at the specified value of λ differs significantly from the experimental curve (Fig. 3).

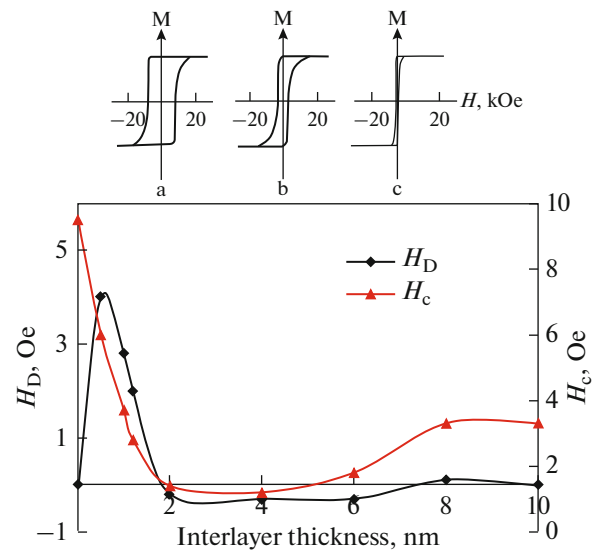


Fig. 4. The upper part includes the hysteresis loops for different interlayer thicknesses: (a) 0, (b) 0.6, and (c) 2 nm. The lower part is the dependences of the dipole coupling field and the coercive force of CoP(amorphous)/NiP/CoP(amorphous) films on the interlayer thickness.

As follows from [4], imperfections in the interlayer in three-layer films that are due to the film discontinuity and different thicknesses over the film area have a strong effect on the coercive force. It is shown that the region of the interlayer thicknesses, where a sharp decrease of H_c is observed, depends on the processes of diffusion of atoms at the boundary of the contacting layers. It follows from [18] that Co–P alloys in the amorphous and crystalline phases have different degrees of atomic ordering, while the atomic diffusion processes are possible only in the amorphous phase. As follows from Figs. 3 and 4, a sharp decrease in the H_D and H_c values occurs in the same interval of the interlayer thicknesses in films with different structures of the lower layers made of crystalline or amorphous Co–P alloys.

Therefore, for the sake of completeness of the explanation, it is proposed to consider the last of the types of interactions discussed here, for which the short-acting local exchange between atoms of the paramagnetic layer and atoms of ferromagnetic layers is responsible. The characteristic radius of this interaction is on the order of a dozen of interatomic distances.

Let us use an approach based on solving the Landau–Ginzburg equation to quantitatively estimate the dipole coupling field H_D [19–21]. The essence of this method is to represent the free-energy functional as an expansion in terms of the order parameter, the role of which is played by the local magnetization M . The

magnetic energy of the paramagnetic layer can be represented as:

$$\begin{aligned} E &= \frac{1}{2} \int \left[\frac{J_1}{a} (\nabla M)^2 + \frac{J_2}{a^3} M^2 \right] dV \\ &= \frac{1}{2} S \int \left[\frac{J_1}{a} (\nabla M)^2 + \frac{J_2}{a^3} M^2 \right] dx, \end{aligned} \quad (2)$$

where S is the area of the interface between the layers, J_1 is the interatomic-exchange constant, a is the interatomic distance, J_2 is the intraatomic-exchange constant, and M is the local magnetization. The integration (2) should be performed over the volume of the paramagnetic layer. In our case, $t \ll \sqrt{S}$; hence, the calculation can be reduced to a single integral over the x coordinate.

The following function satisfies the Euler–Lagrange equation for functional (2):

$$M(x) = m_{01} e^{\xi x} + m_{02} e^{-\xi x}, \quad (3)$$

where the constants m_{01} and m_{02} are determined from the boundary conditions.

To estimate the effective parameter of the exchange coupling between the magnetic subsystems of the ferromagnetic layers, two extreme cases are considered: (1) the magnetizations of the magnetic layers are oriented in parallel, (2) the magnetizations are oriented antiparallel. For these cases, the boundary conditions take the form:

$$M\left(\pm \frac{t}{2}\right) = M_0, \quad M\left(\pm \frac{t}{2}\right) = \pm M_0. \quad (4)$$

The distributions of the magnetization in the paramagnetic layer for these cases, respectively, take the form ($\xi^2 = J_2/J_1 a^2$):

$$M_{\text{fm}} = M_0 \frac{\cosh(\xi x)}{\cosh\left(\xi \frac{t}{2}\right)}; \quad M_{\text{afm}} = M_0 \frac{\sinh(\xi x)}{\sinh\left(\xi \frac{t}{2}\right)}. \quad (5)$$

The following expressions for the energies from (1) are then obtained:

$$\begin{aligned} E_{\text{fm}} &= \frac{S J_1 \xi M_0^2}{a} \tanh\left(\xi \frac{t}{2}\right); \\ E_{\text{afm}} &= \frac{S J_1 \xi M_0^2}{a} \frac{1}{\tanh\left(\xi \frac{t}{2}\right)}. \end{aligned} \quad (6)$$

The effective exchange constant is estimated from the relationship:

$$\begin{aligned} J_{\text{eff}} &= \frac{E_{\text{eff}}}{S} \approx E_{\text{afm}} - E_{\text{fm}} \\ &= \frac{J_1 \xi M_0^2}{a} \left[\frac{1}{\tanh\left(\xi \frac{t}{2}\right)} - \tanh\left(\xi \frac{t}{2}\right) \right] = \frac{2 J_1 \xi M_0^2}{a \sinh(\xi t)}. \end{aligned} \quad (7)$$

In view of (7), the following estimate for the dipole coupling field is obtained:

$$H_D(t) = \frac{J_{\text{eff}}}{M_0 t_f} \approx \frac{2 J_1 \xi M_0}{t_f a} \frac{1}{\sinh(\xi t)}. \quad (8)$$

The dependence of H_D on the interlayer thickness determined by Eq. (8), is qualitatively consistent with the experimental results (see Fig. 3). There is also a quantitative agreement. In fact, the parameter ξ has an order of $1/a$ [20, 21]; for nickel compounds, $\xi \approx 1/0.35 \text{ nm}^{-1}$. The characteristic width of the paramagnetic layer t_0 , on which the field H_D decreases approximately by a factor of three, is determined from the equation: $\sinh(\xi t_0) = 3$. In this case, $t_0 \approx 0.64 \text{ nm}$, which is in good agreement with the measurement results.

CONCLUSIONS

The interaction of ferromagnetic layers in the proposed mechanism has the character of an effective exchange that occurs due to the short-range interaction between the nearest atoms in the paramagnetic layer. Despite the short-range and weak nature of this interaction, a large number of atoms involved in the bonds at the ferromagnetic–paramagnetic interface makes this interaction noticeable, and the ferromagnetic nature leads to a dipole coupling field of the hysteresis loop.

It should be noted that in the system under consideration, the influence of imperfections in the interlayer cannot be excluded. To determine which of the two mechanisms is predominant in the region of the interlayer thicknesses, where there is a sharp decline in both the dipole coupling field and the coercive force, additional research is required.

ACKNOWLEDGMENTS

We are grateful to S.Ya. Kiparisov for the provided samples.

FUNDING

This work was supported by ongoing institutional funding. No additional grants to carry out or direct this particular research were obtained.

CONFLICT OF INTEREST

The authors of this work declare that they have no conflicts of interest.

REFERENCES

1. G. Binasch, P. Grünberg, F. Saurenbach, and W. Zinn, “Enhanced magnetoresistance in layered magnetic structures with antiferromagnetic interlayer exchange,”

- Phys. Rev. B **39**, 4828–4830 (1989).
<https://doi.org/10.1103/physrevb.39.4828>
2. E. B. Myers, D. C. Ralph, J. A. Katine, R. N. Louie, and R. A. Buhrman, “Current-induced switching of domains in magnetic multilayer devices,” *Science* **285**, 867–870 (1999).
<https://doi.org/10.1126/science.285.5429.867>
 3. Y. Pennec, J. Camarero, J. C. Toussaint, S. Pizzini, M. Bonfim, F. Petroff, W. Kuch, F. Offi, K. Fukumoto, F. Nguyen Van Dau, and J. Vogel, “Switching-mode-dependent magnetic interlayer coupling strength in spin valves and magnetic tunnel junctions,” *Phys. Rev. B* **69**, 180402–180403 (2004).
<https://doi.org/10.1103/physrevb.69.180402>
 4. V. O. Vas’kovskii, P. A. Savin, V. N. Lepalovskii, G. S. Kandaurova, and Yu. M. Yarmoshenko, “Hysteretic properties and domain structure of the layered magnetic films,” *Phys. Met. Metallogr.* **79**, 282–286 (1995).
 5. V. O. Vas’kovskii and V. N. Lepalovskij, “Magnetization reversal features of Fe₁₅Co₂₀Ni₆₅ sandwiches with various anisotropy of layers,” *J. Phys. IV France* **8**, 441–444 (1998).
<https://doi.org/10.1051/jp4:19982103>
 6. S. R. Herd and K. Y. Ahn, “Magnetic domain structures in multilayered NiFe films,” *J. Appl. Phys.* **50**, 2384–2386 (1979).
<https://doi.org/10.1063/1.326960>
 7. A. Gayen, K. Umadevi, A. Chelvane J, and P. Alagar-samy, “Tuning magnetic properties of thick CoFeB film by interlayer coupling in trilayer structured thin films,” *J. Mater. Sci. Eng.* **7**, 1000437 (2018).
<https://doi.org/10.4172/2169-0022.1000437>
 8. M. K. Kazimierczuk, *High-Frequency Magnetic Components*, 2nd ed. (John Wiley & Sons, 2014).
<https://doi.org/10.1002/9781118717806>
 9. A. V. Chzhan, S. A. Podorozhnyak, A. N. Shahov, D. A. Velikanov, and G. S. Patrin, “Thickness dependences of coercivity in three layer films obtained by chemical deposition,” *J. Phys.: Conf. Ser.* **1389**, 012118 (2019).
<https://doi.org/10.1088/1742-6596/1389/1/012118>
 10. V. V. Bondar’, *Electrochemistry-1966* (VINITI, Moscow, 1968).
 11. M. N. Volochaev, M. S. Shcheglova, Yu. Yu. Balashov, and Yu. Yu. Loginov, “Features of large-scale thin foils fabrication for transmission electron microscopy by focused ion beam,” *IOP Conf. Ser.: Mater. Sci. Eng.* **822**, 012028 (2020).
<https://doi.org/10.1088/1757-899x/822/1/012028>
 12. V. V. Polyakov, K. P. Polyakova, V. A. Seredkin, G. S. Patrin, and G. V. Bondarenko, “Magneto-optical properties of nanogranulated Co–Ti–O films,” *Bull. Russ. Acad. Sci.: Phys.* **75**, 1106–1107 (2011).
<https://doi.org/10.3103/s1062873811080302>
 13. L. Neel, “Sur un nouveau monde de couplage entre les aimantations de deux couches minces ferromagnétiques,” *C. R. Acad. Sci. D* **255**, 1676–1681 (1962).
<https://hal.science/hal-02878443>.
 14. D. Edwards, J. Mathon, and E. P. Wohlfarth, “A phenomenological theory of strongly paramagnetic and weakly ferromagnetic dilute alloys,” *J. Phys. F: Met. Phys.* **5**, 1619–1624 (1975).
<https://doi.org/10.1088/0305-4608/5/8/020>
 15. J. Mathon, “Magnetisation of a strongly paramagnetic layer in contact with a ferromagnetic substrate,” *J. Phys. F: Met. Phys.* **16**, L217–L221 (1986).
<https://doi.org/10.1088/0305-4608/16/9/003>
 16. B. D. Schrag, A. Anguelouch, S. Ingvarsson, G. Xiao, Yu. Lu, P. L. Trouilloud, A. Gupta, R. A. Wanner, W. J. Gallagher, P. M. Rice, and S. S. Parkin, “Néel ‘orange-peel’ coupling in magnetic tunneling junction devices,” *Appl. Phys. Lett.* **77**, 2373–2375 (2000).
<https://doi.org/10.1063/1.1315633>
 17. S. Tegen, I. Mönch, J. Schumann, H. Vinzelberg, and C. Schneider, “Effect of Néel coupling on magnetic tunnel junctions,” *J. Appl. Phys.* **89**, 8169–8174 (2001).
<https://doi.org/10.1063/1.1365445>
 18. A. V. Chzhan, S. A. Podorozhnyak, S. M. Zharkov, S. A. Gromilov, and G. S. Patrin, “Induced magnetic anisotropy of Co–P thin films obtained by electroless deposition,” *J. Magn. Magn. Mater.* **537**, 168129 (2021).
<https://doi.org/10.1016/j.jmmm.2021.168129>
 19. R. Skomski, T. Komesu, H.-K. Jeong, C. N. Borca, P. A. Dowben, D. Ristoiu, and J. P. Nozieres, “A Landau–Ginzburg description of Sb overlayers,” *MRS Online Proc. Libr.* **674**, 710 (2001).
<https://doi.org/10.1557/proc-674-u7.10>
 20. P. A. Dowben, W. W. Hürsch, and M. Landolt, “The experimentally determined thin-film limit to the Ginzburg–Landau model of thin-film magnetism,” *J. Magn. Magn. Mater.* **125**, 120–124 (1993).
[https://doi.org/10.1016/0304-8853\(93\)90826-n](https://doi.org/10.1016/0304-8853(93)90826-n)
 21. I. I. Oleinik, E. Y. Tsybal, and D. G. Pettifor, “Structural and electronic properties of Co/Al₂O₃/Co magnetic tunnel junction from first principles,” *Phys. Rev. B* **62**, 3952–3959 (2000).
<https://doi.org/10.1103/physrevb.62.3952>

Translated by A. Seferov

Publisher’s Note. Pleiades Publishing remains neutral with regard to jurisdictional claims in published maps and institutional affiliations.